

# 考虑表面效应的功能梯度夹层纳米板 屈曲和后屈曲研究\*

肖俊华<sup>1,2\*\*</sup> 王 杰<sup>1,2,3,4</sup>

(<sup>1</sup> 燕山大学工程力学系, 秦皇岛, 066004)(<sup>2</sup> 燕山大学河北省重型装备与大型结构力学可靠性重点实验室, 秦皇岛, 066004)

(<sup>3</sup> 中科院力学研究所非线性力学国家重点实验室, 北京, 100190)(<sup>4</sup> 中国科学院大学工程科学学院, 北京, 100049)

**摘要** 功能梯度材料制成的微纳结构元件的力学性能不同于常规材料制成的宏观结构. 本文基于 Kirchhoff 板理论以及考虑剪切变形的 Mindlin 板理论, 研究了表面效应影响下功能梯度夹层纳米板的屈曲和后屈曲行为. 通过平衡分析导出了屈曲和后屈曲的控制方程, 得到了单轴和双轴压缩下临界屈曲载荷的解析解. 利用 Galerkin 方法, 给出了加载边可动和不可动两种边界条件下临界后屈曲载荷解答. 数值结果表明, 表面效应对功能梯度纳米层合板稳定性的影响与组成板的材料的体积分数有关, 也与结构表面积与体积的比值有关. 考虑剪切变形会减小功能梯度纳米层合板的屈曲和后屈曲的临界载荷; 对于较薄纳米层合板可以忽略剪切变形的影响.

**关键词** 表面效应, 功能梯度材料, 矩形层合板, 屈曲, 后屈曲

**DOI:** 10.19636/j.cnki.cjsm42-1250/o3.2024.062

## 0 引言

纳米板结构由于优异的力学性能广泛应用于纳米机电系统(NEMS)<sup>[1]</sup>. 纳米结构的比表面积(表面积与体积比值)非常高. 同体积时, 纳米层合板的比表面积远大单层纳米材料的比表面积, 表面效应更为显著. 表面效应产生的原因在于纳米结构表面层附近原子与块体原子处于不同的环境条件中. 经典板壳理论没有考虑表面效应, 不再适用于描述纳米板壳等纳米结构<sup>[2]</sup>. 为了描述表面效应对纳米结构力学性能的影响, Gurtin 和 Murdoch<sup>[3-5]</sup> 提出了考虑表面效应的表面弹性模型, 该模型将固体表面层假设为数学上零厚度的薄膜, 表面层薄膜与底层体部分紧密贴合在一起且具有与体部分不同的材料特性.

表面效应对纳米结构的影响可以看作是表面弹性和表面残余应力的结合<sup>[6]</sup>, 其中表面弹性的影响可以用表面拉梅常数来表示. 为了计算方便, 同种材

料组成的纳米板上下表面层的表面参数通常被假设为相同的. 表面参数通常与材料属性相关, 不同材料的表面参数有着明显区别. 经典板壳理论忽略了表面法向应力, 由于考虑表面效应引入了新的参数, 为了考虑表面的平衡, 也需要考虑表面层的法向应力. Barati 和 Zenkour<sup>[7]</sup> 同时考虑挠曲电效应和表面效应分析了存在几何缺陷的压电纳米梁的后屈曲特性, 其中挠曲电效应产生的原因在于电极化和应变梯度之间的耦合, 基于哈密顿原理, 求出了控制方程和边界条件并利用 Galerkin 方法求解, 得到的数值结果表明, 挠曲电性和表面效应对系统的后屈曲有显著影响, 此外, 屈曲后的温度也与施加的电压以及残余应力有关. 之后 Abbasi 和 Ghassemi<sup>[8]</sup> 将非局部理论与表面弹性理论相结合, 发展了一种由压电材料组成了纳米板模型并利用该模型研究了压电纳米板的弯曲行为. Hosseini 等<sup>[9]</sup> 基于表面弹性理论, 利用哈密顿原理得到了纳米板的控制方程以及相应边界条件下挠度的解析解, 得到的结果表明固有频

\* 河北省自然科学基金项目(A2022203025)资助.

2024-12-30 收到修改稿, 2025-01-02 网络首发.

\*\* 通讯作者. E-mail: xiaojunhua@ysu.edu.cn.

率会在表面弹性模量的影响下发生变化. Rafieian 等<sup>[10]</sup>研究了表面能和温度对弹性地基上双压电纳米板屈曲的影响,利用虚功原理导出了控制方程,并利用有限差分法求解,他们研究发现通过增加外部电压,表面应力对屈曲的影响得到增强. 基于 Gurtin-Murdoch 表面弹性理论和 Kirchhoff 板模型, Kamali 和 Shahabian<sup>[11]</sup>提出了一种新的尺寸相关公式,用于描述嵌入弹性基地中的对称多孔纳米薄板的屈曲和后屈曲行为,利用哈密顿原理推导了相应边界条件下的控制方程,考虑了双轴压缩、单轴压缩以及纯剪切三种情况下简支多孔纳米板的后屈曲行为.

功能梯度材料作为一种新型复合材料受到研究人员越来越多的关注. 由于组成材料成分的变化,用功能梯度材料制成的微纳米结构元件的力学响应与用常规材料制成的小尺寸结构元件不同<sup>[12]</sup>. 板状结构是微纳米机电系统中的基本元件,因此研究由功能梯度材料制成的板的力学性能是十分必要. Ke 等<sup>[13]</sup>使用微分求积法得到了微纳米尺度下功能梯度环形板的弯曲、屈曲和自由振动. 关于研究功能梯度材料的建模大致分为三种,其中一种为 Voigt 模型<sup>[14]</sup>,该模型使用混合规则,是一种最简单的建模方式,应用广泛但是准确度有限;另一种为 Mori-Tanaka 模型<sup>[15]</sup>,该模型适合于功能梯度材料是连续的基质和不连续夹杂组成的混合物,但该模型未考虑材料的有效质量密度;还有一种模型为自洽模型<sup>[16]</sup>,该模型适合于含骨骼微结构的功能梯度材料,但该模型也未考虑材料整体的有效质量密度.

关于微纳米板的屈曲和后屈曲行为, Li 等<sup>[17]</sup>研究了石墨烯强化的功能梯度板的固有频率和屈曲行为,在模型中考虑了一阶和三阶剪切变形,并假设板内的孔隙均匀或非均匀地分布在金属基体中,数值研究表明,石墨烯的加入可以有效地提高功能梯度多孔板的刚度. Sahmani 等<sup>[18]</sup>研究了石墨烯强化的功能梯度多孔微/纳米板非线性大振幅振动响应的尺寸依赖性,采用改进的微扰方法,得到了考虑非局部应变梯度的非线性频率的解析表达式,结果表明对于振幅较高的振动,孔隙率对功能梯度微/纳米板非线性频率的显影响增强.

Duan 等<sup>[19]</sup>基于修正的偶应力理论和双变量高

阶剪切变形理论,建立了考虑尺寸效应的微板力学模型,研究了面内载荷、边界条件、纵横比、长厚比、尺寸效应参数等对板屈曲载荷和屈曲模式的影响. 随后,张立民等<sup>[20]</sup>发展了一种层间填充弹性介质的双层微板系统在面内压缩荷载作用下的屈曲模型,运用 Navier 法得到了四边简支时边界条件下,该模型的同步/异步屈曲的解析解. 最近, Duan 等<sup>[21]</sup>基于修正的偶应力理论,研究了在面内剪切和压缩荷载联合作用下斜厚微板的弹性屈曲,数值结果表明,屈曲模式受尺寸效应和倾斜角的组合影响,而不仅仅是屈曲载荷的影响. Li 等<sup>[22]</sup>将 Gurtin-Murdoch 表面理论引入 von Karman 板理论,研究了具有表面效应的梯度多孔圆形纳米板在随动力作用下的非线性后屈曲行为. Momeni 和 Tahani<sup>[23]</sup>基于非局部应变梯度和一阶剪切变形理论,得到了简支和夹紧端条件下纳米板的临界屈曲载荷和后屈曲路径.

本文基于表面弹性理论,发展了一种新的考虑表面效应的功能梯度夹层板模型,利用力平衡分析分别得到了功能梯度夹层板屈曲和后屈曲的控制方程. 考虑单轴压缩和双轴压缩,给出了临界屈曲载荷的解析解,利用 Galerkin 方法给出了加载边可动和加载边不可动时临界后屈曲载荷的近似解. 讨论了板的几何尺寸以及体积分数等对临界屈曲载荷和后屈曲平衡路径的影响.

## 1 功能梯度纳米板模型

图 1 为长度为  $a$ 、宽度为  $b$ 、厚度为  $h$  的由功能梯度材料组成矩形纳米板. 如图 2 所示,上下顶面  $z = z_1, z = z_4$  处富含金属,在  $z = z_2, z = z_3$  处富含陶瓷,中间层是各向同性的均匀陶瓷材料.

功能梯度矩形纳米板体积分数表示为<sup>[24]</sup>:

$$V^{(1)}(z) = \left( \frac{z - z_1}{z_2 - z_1} \right)^n, \quad z \in [z_1, z_2] \quad (1a)$$

$$V^{(2)}(z) = 1, \quad z \in [z_2, z_3] \quad (1b)$$

$$V^{(3)}(z) = \left( \frac{z_4 - z}{z_4 - z_3} \right)^n, \quad z \in [z_3, z_4] \quad (1c)$$

其中  $V^{(i)} (i=1, 2, 3)$  表示第  $i$  层的体积分数,  $n$  表示体积分数指数 ( $0 \leq n < \infty$ ).

功能梯度纳米板的有效杨氏模量由下式

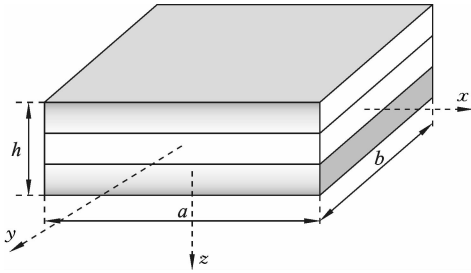


图 1 功能梯度纳米夹层板示意图

Fig. 1 Schematic of the functionally graded sandwich nanoplate

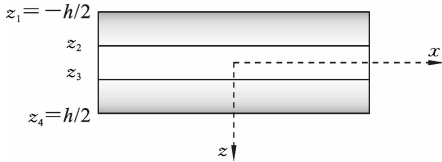


图 2 功能梯度纳米夹层板横截面

Fig. 2 Cross section of the functionally graded sandwich nanoplate

给出<sup>[25]</sup>：

$$E^{(i)}(z) = E_m + (E_c - E_m)V^{(i)} \quad (2)$$

其中  $E^{(i)}(z)$  和表示第  $i$  层的杨氏模量。下标  $m$  和  $c$  分别表示金属和陶瓷成分。纳米板的泊松比  $\mu$  与杨氏模量有类似的表达式。与杨氏模量相比，改变泊松比对功能梯度层合纳米板的影响可以忽略<sup>[26,27]</sup>。因此，在这项工作中假设材料的泊松比保持不变。

对于纳米层合板，表面效应可分为两部分，一部分是表面残余应力，另一部分是表面弹性<sup>[6]</sup>。对于残余应力的影响，根据 Laplace-Yong 方程表示如下<sup>[28]</sup>：

$$q(x, y) = H \left( \frac{\partial^2 w}{\partial x^2} + \frac{\partial^2 w}{\partial y^2} \right) \quad (3)$$

其中  $w$  表示表面的挠度， $H$  取决于残余应力值和结构形状<sup>[29]</sup>。

$$H = \tau_0^+ + \tau_0^- \quad (4)$$

其中  $\tau_0^+$  和  $\tau_0^-$  分别是  $z = z_1$  和  $z = z_4$  处的表面残余应力。

表面弹性的影响可由表面杨氏模量表示。考虑表面效应的等效杨氏模量  $E^*$  为<sup>[30]</sup>：

$$E^* = \frac{1}{h} \left( \int_{z_1}^{z_2} E^1 dz + \int_{z_2}^{z_3} E^2 dz + \int_{z_3}^{z_4} E^3 dz + E^{s+} + E^{s-} \right) \quad (5)$$

其中  $E^{s+}$  和  $E^{s-}$  分别表示  $z = z_1$  和  $z = z_4$  处的表面杨氏模量。由于板的表面可视为弹性薄膜，考虑表面效应的等效弯曲刚度可以表示为<sup>[6]</sup>：

$$D^* = \frac{1}{(1 - \mu^2)} \left( \int_{z_1}^{z_2} E^1 z^2 dz + \int_{z_2}^{z_3} E^2 z^2 dz + \int_{z_3}^{z_4} E^3 z^2 dz \right) + E^{s+} z_1^2 + E^{s-} z_4^2 \quad (6)$$

## 2 功能梯度纳米层合板基本公式

### 2.1 Kirchhoff 板理论

根据 Kirchhoff 板理论，位移分量可写成<sup>[31]</sup>：

$$u = -z \frac{\partial w}{\partial x}, \quad v = -z \frac{\partial w}{\partial y}, \quad w = w(x, y) \quad (7)$$

其中  $w(x, y)$  是层合板的垂直位移。根据式(7)，层合板的应变分量可表示为：

$$\epsilon_x = \frac{\partial u}{\partial x} = -z \frac{\partial^2 w}{\partial x^2}, \quad \epsilon_y = \frac{\partial v}{\partial y} = -z \frac{\partial^2 w}{\partial y^2} \quad (8a)$$

$$\gamma_{xy} = \frac{\partial v}{\partial x} + \frac{\partial u}{\partial y} = -2z \frac{\partial^2 w}{\partial x \partial y}, \quad \gamma_{xz} = \gamma_{yz} = \epsilon_z = 0 \quad (8b)$$

各向同性材料的本构关系由下式给出：

$$\epsilon_x = \frac{(\sigma_x - \mu \sigma_y)}{E}, \quad \epsilon_y = \frac{(\sigma_y - \mu \sigma_x)}{E}, \quad \gamma_{xy} = \frac{\tau_{xy}}{G} \quad (9)$$

其中  $G$  为剪切模量， $\sigma_x, \sigma_y$  和  $\tau_{xy}$  为应力分量。

根据式(8a)，(8b)和(9)，层合板的内力表示为：

$$\begin{cases} M_x = -D \left( \frac{\partial^2 w}{\partial x^2} + \mu \frac{\partial^2 w}{\partial y^2} \right) \\ M_y = -D \left( \frac{\partial^2 w}{\partial y^2} + \mu \frac{\partial^2 w}{\partial x^2} \right) \\ M_{xy} = -D(1 - \mu) \frac{\partial^2 w}{\partial x \partial y} \end{cases} \quad (10a)$$

$$Q_x = -D \frac{\partial}{\partial x} \nabla^2 w, \quad Q_y = -D \frac{\partial}{\partial y} \nabla^2 w \quad (10b)$$

其中  $M_x$  和  $M_y$  是弯矩， $M_{xy}$  是扭矩， $Q_x$  和  $Q_y$  是横向剪切力。考虑受纵向载荷作用时层合板的屈曲，力矩平衡方程可写成<sup>[32]</sup>：

$$\frac{\partial M_x}{\partial x} + \frac{\partial M_{xy}}{\partial y} = Q_x, \quad \frac{\partial M_y}{\partial y} + \frac{\partial M_{xy}}{\partial x} = Q_y \quad (11)$$

层合板的力平衡方程由下式给出<sup>[32]</sup>:

$$\frac{\partial N_x}{\partial x} + \frac{\partial N_{xy}}{\partial y} = 0, \quad \frac{\partial N_y}{\partial y} + \frac{\partial N_{xy}}{\partial x} = 0 \quad (12a)$$

$$\frac{\partial Q_x}{\partial x} + \frac{\partial Q_y}{\partial y} + N_x \frac{\partial^2 w}{\partial x^2} + 2N_{xy} \frac{\partial^2 w}{\partial x \partial y} + N_y \frac{\partial^2 w}{\partial y^2} = 0 \quad (12b)$$

其中  $N_x = h\sigma_x$ ,  $N_y = h\sigma_y$ ,  $N_{xy} = h\tau_{xy}$ . 基于式(10a)-(12b), 得到各向同性层合板在纵向载荷作用下的经典控制方程为:

$$D \nabla^4 w = N_x \frac{\partial^2 w}{\partial x^2} + 2N_{xy} \frac{\partial^2 w}{\partial x \partial y} + N_y \frac{\partial^2 w}{\partial y^2} \quad (13)$$

基于式(3), (6)和(13), 得到考虑表面效应的功能梯度层合纳米板的控制方程:

$$D^* \nabla^4 w = (N_x + H) \frac{\partial^2 w}{\partial x^2} + 2N_{xy} \frac{\partial^2 w}{\partial x \partial y} + (N_y + H) \frac{\partial^2 w}{\partial y^2} + H \left( \frac{\partial^2 w}{\partial x^2} + \frac{\partial^2 w}{\partial y^2} \right) \quad (14)$$

## 2.2 Mindlin 板理论

在 Mindlin 板理论中, 位移分量可以写成<sup>[33]</sup>:

$$u = -z\varphi_x, \quad v = -z\varphi_y, \quad w = w(x, y) \quad (15)$$

其中  $\varphi_x$  和  $\varphi_y$  分别是  $x$  和  $y$  方向上的角位移. 基于式(15), Mindlin 板理论中纳米层合板的应变分量为:

$$\epsilon_x = \frac{\partial u}{\partial x} = -z \frac{\partial \varphi_x}{\partial x}, \quad \epsilon_y = \frac{\partial v}{\partial y} = -z \frac{\partial \varphi_y}{\partial y} \quad (16a)$$

$$\gamma_{xy} = \frac{\partial v}{\partial x} + \frac{\partial u}{\partial y} = -z \left( \frac{\partial \varphi_x}{\partial y} + \frac{\partial \varphi_y}{\partial x} \right) \quad (16b)$$

$$\gamma_{xz} = \frac{\partial w}{\partial x} - \varphi_x, \quad \gamma_{yz} = \frac{\partial w}{\partial y} - \varphi_y, \quad \epsilon_z = 0 \quad (16c)$$

Mindlin 纳米层合板的本构关系与 Kirchhoff 纳米层合板相同. 根据式(9), (16a), (16b)和(16c), Mindlin 纳米层合板的内力表示为:

$$\begin{cases} M_x = -D \left( \frac{\partial \varphi_x}{\partial x} + \mu \frac{\partial \varphi_y}{\partial y} \right) \\ M_y = -D \left( \frac{\partial \varphi_y}{\partial y} + \mu \frac{\partial \varphi_x}{\partial x} \right) \\ M_{xy} = -\frac{D(1-\mu)}{2} \left( \frac{\partial \varphi_x}{\partial y} + \frac{\partial \varphi_y}{\partial x} \right) \end{cases} \quad (17a)$$

$$Q_x = -KhG \left( \frac{\partial w}{\partial x} - \varphi_x \right), \quad Q_y = -KhG \left( \frac{\partial w}{\partial y} - \varphi_y \right) \quad (17b)$$

其中  $K$  为剪切修正系数, 取  $\pi^2/12$ <sup>[34]</sup>. Mindlin 纳米层合板的力矩平衡方程和力平衡方程与 Kirchhoff

纳米层合板相同. 因此, Mindlin 板理论中各向同性纳米层合板在纵向载荷作用下的经典控制方程可通过将式(17a)和(17b)分别代入式(11), (12a)和(12b)中得到:

$$D \nabla^4 w = \left( 1 - \frac{D \nabla^2}{KhG} \right) \left( N_x \frac{\partial^2 w}{\partial x^2} + 2N_{xy} \frac{\partial^2 w}{\partial x \partial y} + N_y \frac{\partial^2 w}{\partial y^2} \right) \quad (18)$$

基于式(3), (6)和(18), 得到考虑表面效应的控制方程为:

$$D^* \nabla^4 w = \left( 1 - \frac{D^* \nabla^2}{KhG^*} \right) \left( (N_x + H) \frac{\partial^2 w}{\partial x^2} + 2N_{xy} \frac{\partial^2 w}{\partial x \partial y} + (N_y + H) \frac{\partial^2 w}{\partial y^2} + H \left( \frac{\partial^2 w}{\partial x^2} + \frac{\partial^2 w}{\partial y^2} \right) \right) \quad (19)$$

## 2.3 功能梯度纳米层合板后屈曲

式(14)和(19)均适用于功能梯度纳米层合板的非线性后屈曲问题, 但此时  $N_x$ ,  $N_y$ , 和  $N_{xy}$  是  $x$  和  $y$  的函数. 引入应力函数  $\Phi$ :

$$\begin{cases} N_x + H = h\sigma_x = h \frac{\partial^2 \Phi}{\partial y^2} \\ N_y + H = h\sigma_y = h \frac{\partial^2 \Phi}{\partial x^2} \\ N_{xy} = h\tau_{xy} = -h \frac{\partial^2 \Phi}{\partial x \partial y} \end{cases} \quad (20)$$

将式(20)代入(14), 可得:

$$D^* \nabla^4 w = h \frac{\partial^2 \Phi}{\partial y^2} \frac{\partial^2 w}{\partial x^2} - 2h \frac{\partial^2 \Phi}{\partial x \partial y} \frac{\partial^2 w}{\partial x \partial y} + h \frac{\partial^2 \Phi}{\partial x^2} \frac{\partial^2 w}{\partial y^2} + H \left( \frac{\partial^2 w}{\partial x^2} + \frac{\partial^2 w}{\partial y^2} \right) \quad (21)$$

将式(20)代入式(19), 得到:

$$D^* \nabla^4 w = \left( 1 - \frac{D^* \nabla^2}{KhG^*} \right) \left( h \frac{\partial^2 \Phi}{\partial y^2} \frac{\partial^2 w}{\partial x^2} - 2h \frac{\partial^2 \Phi}{\partial x \partial y} \frac{\partial^2 w}{\partial x \partial y} + \frac{\partial^2 \Phi}{\partial x^2} \frac{\partial^2 w}{\partial y^2} + H \left( \frac{\partial^2 w}{\partial x^2} + \frac{\partial^2 w}{\partial y^2} \right) \right) \quad (22)$$

Von-Kármán 非线性应变位移关系可以写为<sup>[30]</sup>:

$$\begin{cases} \epsilon_x = \frac{\partial u}{\partial x} + \frac{1}{2} \left( \frac{\partial w}{\partial x} \right)^2 \\ \epsilon_y = \frac{\partial v}{\partial y} + \frac{1}{2} \left( \frac{\partial w}{\partial y} \right)^2 \\ \gamma_{xy} = \frac{\partial v}{\partial x} + \frac{\partial u}{\partial y} + \frac{\partial w}{\partial x} \frac{\partial w}{\partial y} \end{cases} \quad (23)$$

基于式(5), (9), (20)和(23), 考虑表面效应的相容方程可以写为:

$$\nabla^4 \Phi = E^* \left( \left( \frac{\partial^2 \omega}{\partial x \partial y} \right)^2 - \frac{\partial^2 \omega}{\partial x^2} \frac{\partial^2 \omega}{\partial y^2} \right) \quad (24)$$

式(24)适用于 Kirchhoff 和 Mindlin 纳米层合板。

### 3 两种板理论求解

#### 3.1 功能梯度纳米层合板屈曲解析解

考虑四边简支边界条件下的功能梯度纳米层合板,在  $x = -\frac{a}{2}$  和  $x = \frac{a}{2}$  两边受到均布压力  $P_x$  作用,此时  $N_x$ ,  $N_y$  和  $N_{xy}$  分别表示如下:

$$N_x + H = -P_x, \quad N_y + H = 0, \quad N_{xy} = 0 \quad (25)$$

将式(25)代入(14),Kirchhoff 板理论下的控制方程改写为:

$$D^* \nabla^4 \omega = -P_x \frac{\partial^2 \omega}{\partial x^2} + H \left( \frac{\partial^2 \omega}{\partial x^2} + \frac{\partial^2 \omega}{\partial y^2} \right) \quad (26)$$

四边简支的边界条件表示为:

$$(W)_{x=0,a} = 0; \quad (W)_{y=0,b} = 0 \quad (27a)$$

$$\left( \frac{\partial^2 W}{\partial x^2} \right)_{x=0,a} = 0; \quad \left( \frac{\partial^2 W}{\partial y^2} \right)_{y=0,b} = 0 \quad (27b)$$

基于式(27a)和(27b),横向位移  $\omega$  表示为:

$$\omega = \sum_{m=1}^{\infty} \sum_{l=1}^{\infty} A_{ml} \sin \frac{m\pi x}{a} \sin \frac{l\pi y}{b} \quad (28)$$

其中  $A_{ml}$  是待定系数,  $m$  是  $x$  方向的屈曲半波数,  $l$  是  $y$  方向的屈曲半波数. 将式(28)代入(26),可得:

$$\sum_{m=1}^{\infty} \sum_{l=1}^{\infty} A_{ml} \left[ D^* \left( \frac{m^2 \pi^2}{a^2} + \frac{l^2 \pi^2}{b^2} \right)^2 - P_x \frac{m^2 \pi^2}{a^2} + H \left( \frac{m^2 \pi^2}{a^2} + \frac{l^2 \pi^2}{b^2} \right) \right] \sin \frac{m\pi x}{a} \sin \frac{l\pi y}{b} = 0 \quad (29)$$

基于式(29)可得  $P_x$  表达式如下:

$$P_x = \frac{a^2 \pi^2 D^*}{m^2} \left( \frac{m^2 \pi^2}{a^2} + \frac{l^2 \pi^2}{b^2} \right)^2 + \frac{a^2 H}{m^2} \left( \frac{m^2 \pi^2}{a^2} + \frac{l^2 \pi^2}{b^2} \right) \quad (30)$$

当  $l=1$  可得临界载荷:

$$(P_x)_{cr} = \frac{\pi^2 D^*}{b^2} \left( \frac{m}{a} + \frac{\alpha}{m} \right)^2 + H \left( 1 + \frac{\alpha^2}{m^2} \right) \quad (31)$$

其中  $\alpha = a/b$ . 当纳米层合板在  $y = -\frac{b}{2}$  和  $y = \frac{b}{2}$  两边同样受到大小为  $P_x$  的均布载荷时,式(25)可以改写为:

$$N_x + H = -P_x, \quad N_y + H = -P_x, \quad N_{xy} = 0 \quad (32)$$

基于式(14),(28)和(32),可得:

$$(P_x)_{cr} = \frac{\pi^2 D^*}{b^2} \left( 1 + \frac{1}{\alpha^2} \right) \quad (33)$$

与 Kirchhoff 纳米板相似,Mindlin 板理论下单轴压缩临界载荷表达式可以写为如下形式:

$$(P_x)_{cr} = \frac{\pi^2 D^*}{b^2} \left( 1 + \frac{H}{ktG^*} \right) \left( \frac{m}{\alpha} + \frac{\alpha}{m} \right)^2 + H \left( 1 + \frac{\alpha^2}{m^2} \right) \frac{1 + \frac{\pi^2 D^*}{KhG^* b^2} \left( 1 + \frac{m^2}{\alpha^2} \right)}{1 + \frac{\pi^2 D^*}{KhG^* b^2} \left( 1 + \frac{m^2}{\alpha^2} \right)} \quad (34)$$

双轴压缩下临界载荷表达式可以写为:

$$(P_x)_{cr} = H + \frac{\pi^2 D^*}{b^2} \left( 1 + \frac{1}{\alpha^2} \right) \frac{1 + \frac{\pi^2 D^*}{KhG^* b^2} \left( 1 + \frac{1}{\alpha^2} \right)}{1 + \frac{\pi^2 D^*}{KhG^* b^2} \left( 1 + \frac{1}{\alpha^2} \right)} \quad (35)$$

#### 3.2 功能梯度纳米层合板后屈曲近似解

由于很难得到纳米层合板后屈曲的精确解,因此本文用 Galerkin 方法<sup>[34]</sup>求解近似解. 首先利用 Kirchhoff 板理论,研究四边简支条件下功能梯度纳米层合板,板在  $x = \frac{a}{2}$  和  $x = -\frac{a}{2}$  两边受压,此时挠度的表达式可以写为<sup>[34]</sup>:

$$\omega = f \sin \frac{\pi x}{a} \sin \frac{\pi y}{b} \quad (36)$$

其中,待定系数  $f$  表示纳米层合板中心点的挠度. 将式(36)代入(24)可得:

$$\nabla^4 \Phi = \frac{E^* f^2 \pi^4}{2a^2 b^2} \left( \cos \frac{2\pi x}{a} + \cos \frac{2\pi y}{b} \right) \quad (37)$$

式(37)的解可以写为:

$$\Phi = \Phi_0 + \Phi_p \quad (38)$$

其中  $\Phi_0$  是  $\nabla^4 \Phi = 0$  的通解,可以写为任意的双调和函数:

$$\Phi_0 = -\frac{1}{2h} p_x y^2 - \frac{1}{2h} p_y x^2 \quad (39)$$

其中  $p_y$  是沿  $y$  轴方向的压缩力.  $\Phi_p$  是式(37)的特解:

$$\Phi_p = A \cos \frac{2\pi x}{a} + B \cos \frac{2\pi y}{b} \quad (40)$$

基于式(39)和(40),可以得到:

$$\Phi = \frac{E^* f^2}{32} \left[ \left( \frac{a}{b} \right)^2 \cos \frac{2\pi x}{a} + \left( \frac{b}{a} \right)^2 \cos \frac{2\pi y}{b} \right] - \frac{1}{2h} p_x y^2 - \frac{1}{2h} p_y x^2 \quad (41)$$

将式(41)代入(20),得到各应力表达式:

$$\sigma_x = \frac{\partial^2 \Phi}{\partial y^2} = -E^* \frac{\pi^2}{8} \left(\frac{f}{a}\right)^2 \cos \frac{2\pi y}{b} - \frac{P_x}{h} \quad (42a)$$

$$\sigma_y = \frac{\partial^2 \Phi}{\partial x^2} = -E^* \frac{\pi^2}{8} \left(\frac{f}{a}\right)^2 \cos \frac{2\pi x}{b} - \frac{P_y}{h} \quad (42b)$$

$$\tau_{xy} = -\frac{\partial^2 \Phi}{\partial x \partial y} = 0 \quad (42c)$$

利用 Galerkin 法求解式(21),可得:

$$\int_0^a \int_0^b \left[ D^* \nabla^4 w - h \frac{\partial^2 \Phi}{\partial y^2} \frac{\partial^2 w}{\partial x^2} + 2h \frac{\partial^2 \Phi}{\partial x \partial y} \frac{\partial^2 w}{\partial x \partial y} - h \frac{\partial^2 \Phi}{\partial x^2} \frac{\partial^2 w}{\partial y^2} - H \left( \frac{\partial^2 w}{\partial x^2} + \frac{\partial^2 w}{\partial y^2} \right) \right] \sin \frac{\pi x}{a} \sin \frac{\pi y}{b} dx dy = 0 \quad (43)$$

将式(42a)-(42c)代入(43)中得到:

$$\frac{P_x}{\alpha^2} + P_y = \frac{D^* \pi^2}{b^2} \left(1 + \frac{1}{\alpha^2}\right)^2 + \frac{E^* h \pi^2 f^2}{16b^2} \left(1 + \frac{1}{\alpha^4}\right) + H \left(1 + \frac{1}{\alpha^2}\right) \quad (44)$$

情况一:未加载边  $y = \frac{b}{2}$  和  $y = -\frac{b}{2}$  是可动的.

此时,  $P_y = 0$ , 代入式(44)得:

$$(P_x)_{cr} = \frac{D^* \pi^2}{b^2} \left(\frac{1}{\alpha} + \alpha\right)^2 + \frac{E^* h \pi^2 f^2}{16b^2} \left(\frac{1}{\alpha^2} + \alpha^2\right) + H(1 + \alpha^2) \quad (45)$$

当  $f=0$  且  $m=1$  时,式(45)与(31)是相同的.

情况二:未加载边  $y = \frac{b}{2}$  和  $y = -\frac{b}{2}$  是固定不可动的.

在这种条件下,平行于  $y$  轴的任意纤维的缩短量都为零,即  $\Delta y = 0$ . 因此有:

$$\Delta y = - \left[ \frac{1}{2} \int_0^b \left(\frac{\partial w}{\partial y}\right)^2 dy - \int_0^b \frac{1}{E} (\sigma_x - \mu \sigma_y) dy \right] \quad (46)$$

将式(42a)-(42c)分别代入(44)和(46)中可得:

$$(P_x)_{cr} = \frac{D^* \pi^2}{b^2} \frac{\left(\frac{1}{\alpha} + \alpha\right)^2}{1 + \mu \alpha^2} + \frac{E^* h \pi^2 f^2}{16b^2} \frac{\frac{1}{\alpha^2} + 3\alpha^2}{1 + \mu \alpha^2} + H \frac{1 + \alpha^2}{1 + \mu \alpha^2} \quad (47)$$

考虑 Mindlin 板理论,得到 Galerkin 方程如下:

$$\int_0^a \int_0^b \left[ D^* \nabla^4 w - \left(1 - \frac{D^* \nabla^2}{khG^*}\right) \times \left( h \frac{\partial^2 \Phi}{\partial y^2} \frac{\partial^2 w}{\partial x^2} - 2h \frac{\partial^2 \Phi}{\partial x \partial y} \frac{\partial^2 w}{\partial x \partial y} + \frac{\partial^2 \Phi}{\partial x^2} \frac{\partial^2 w}{\partial y^2} + H \left( \frac{\partial^2 w}{\partial x^2} + \frac{\partial^2 w}{\partial y^2} \right) \right) \right] \sin \frac{\pi x}{a} \sin \frac{\pi y}{b} dx dy = 0 \quad (48)$$

将式(42a)-(42c)代入(48)中,可得:

$$\frac{P_x}{\alpha^2} + P_y = \frac{\frac{D^* \pi^2}{b^2} \left(1 + \frac{1}{\alpha^2}\right)^2}{1 + \frac{D^* \pi^2}{KhGb^2} \left(1 + \frac{1}{\alpha^2}\right)} + \frac{E^* h \pi^2 f^2}{16b^2} \left(1 + \frac{1}{\alpha^4}\right) + H \left(1 + \frac{1}{\alpha^2}\right) \quad (49)$$

情况一:未加载边  $y = \frac{b}{2}$  和  $y = -\frac{b}{2}$  是可动的.

基于式(49)可得此时临界载荷为:

$$(P_x)_{cr} = \frac{\frac{D^* \pi^2}{b^2} \left(\alpha + \frac{1}{\alpha}\right)^2}{1 + \frac{D^* \pi^2}{KhGb^2} \left(1 + \frac{1}{\alpha^2}\right)} + \frac{E^* h \pi^2 f^2}{16b^2} \left(\alpha^2 + \frac{1}{\alpha^2}\right) + H(1 + \alpha^2) \quad (50)$$

当  $f=0$  且  $m=1$  时,式(50)与(34)是相等的.

情况二:未加载边  $y = \frac{b}{2}$  和  $y = -\frac{b}{2}$  是不可动的.

在这种条件下,平行于  $y$  轴的任意纤维的缩短量都为零,即  $y=0$ . 此时临界载荷为:

$$(P_x)_{cr} = \frac{\frac{D^* \pi^2}{b^2(1 + \mu \alpha^2)} \left(\alpha + \frac{1}{\alpha}\right)^2}{1 + \frac{D^* \pi^2}{KhGb^2} \left(1 + \frac{1}{\alpha^2}\right)} + \frac{E^* h \pi^2 f^2 \left(3\alpha^2 + \frac{1}{\alpha^2}\right)}{16b^2(1 + \mu \alpha^2)} + H \frac{(1 + \alpha^2)}{(1 + \mu \alpha^2)} \quad (51)$$

## 4 结果与讨论

研究表面效应对功能梯度纳米板屈曲和后屈曲的影响,选择 Al 为金属材料,选择 Si 为陶瓷材料. Al 和 Si 材料参数见表 1. 两种材料泊松比  $\mu$  均为 0.3. Al 的表面参数为<sup>[35]</sup>:表面杨氏模量  $E^s = 6.09$  N/m,表面残余应力  $\tau^s = 0.9108$  N/m. 每层的厚度均相等.

表 1 Al 和 Si 材料参数<sup>[35]</sup>

Table 1 Material parameters of Al and Si

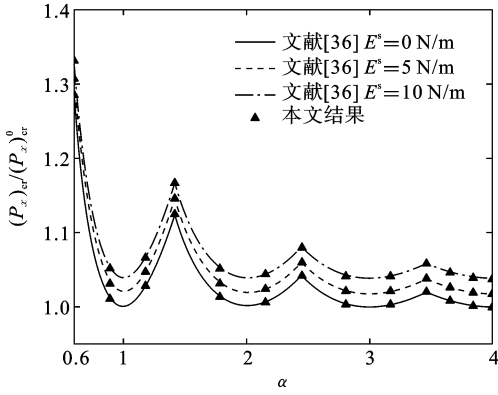
材料	$E(\text{GPa})$	$\rho(\text{kg/m}^3)$
Al	70	2700
Si	210	2331

### 4.1 结果的验证

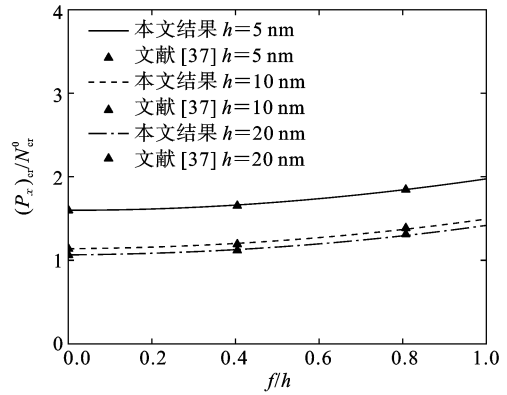
当  $n = \infty$  时,图 1 所示的功能梯度纳米夹层板

的模型可以简化为均质各向同性的三层纳米层合板. 图 3(a)是得到的三层均质纳米层合板临界屈曲和后屈曲载荷结果文献[36]对比图, 其中  $(P_x)_{cr}^0$  表示不考虑表面效应的临界屈曲载荷. 从图中可以看

出, 本文所得结果与文献[36]结果具有良好的一致性. 此外, 将本文夹层板退化为单层均质各向同性板, 所得后屈曲载荷与文献[37]对比见图 3(b), 进一步验证了本文结果的正确性.



(a) 单轴压缩下屈曲载荷对比 ( $b=200 \text{ nm}, h=20 \text{ nm}$ )  
(a) Comparison of buckling loads under uniaxial compression ( $b=200 \text{ nm}, h=20 \text{ nm}$ )



(b) 可动边界条件下后屈曲载荷对比 ( $a=b=15 h$ )  
(b) Comparison of post-buckling loads under moving boundary conditions ( $a=b=15 h$ )

图 3 本文结果与已有结果的对比

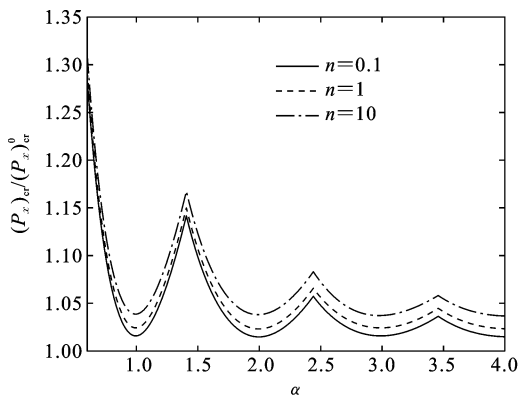
Fig. 3 The contrast between present results and available results

#### 4.2 功能梯度纳米层合板屈曲

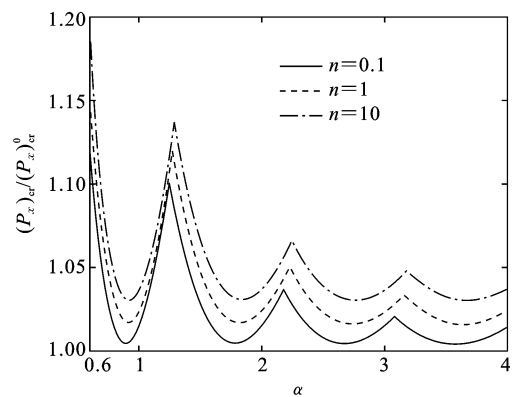
本节通过给出一些数值计算结果, 研究材料体积分数和板的几何尺寸对功能梯度矩形纳米层合板屈曲响应的影响. 临界屈曲载荷通过参数  $(P_x)_{cr}^0$  归一化,  $(P_x)_{cr}^0$  表示不考虑表面效应的临界屈曲载荷.

图 4 给出了单轴压缩条件下, 具有不同体积分数的功能梯度纳米板临界屈曲载荷随长宽比  $\alpha$  的变

化图. 从图中可以看出,  $x$  方向屈曲的波数在增加. 但在  $y$  方向上, 对于任何长宽比, 屈曲的波数始终为  $l=1$ . 此外由图可知, 对于两种功能梯度纳米层合板, 随着体积分数  $n$  增加, 归一化临界屈曲载荷的值增大, 这是因为夹层纳米板中金属成分增加了, 使得表面效应对板整体刚度的影响增强.



(a) Kirchhoff 纳米层合板  
(a) Kirchhoff nanolaminates



(b) Mindlin 纳米层合板  
(b) Mindlin nanolaminates

图 4 单轴压缩下不同体积分数的对归一化屈曲载荷的影响 ( $b=100 \text{ nm}, h=20 \text{ nm}$ )

Fig. 4 Effects of different volume fractions on normalized buckling loads under uniaxial compression ( $b=100 \text{ nm}, h=20 \text{ nm}$ )

图 5 给出了双轴压缩条件下,具有不同体积分数的功能梯度纳米板临界屈曲载荷随长宽比  $\alpha$  的变化图.由图可知,两种层合板的屈曲波数均为  $m=l$

$=1$ .与单轴压缩的情况类似,随着体积分分数  $n$  增加,归一化临界屈曲载荷增加.

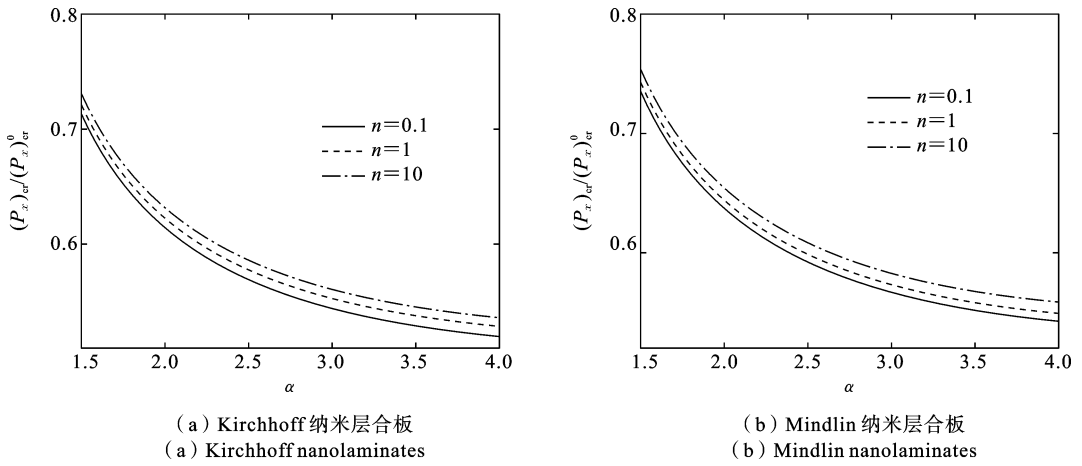


图 5 双轴压缩下不同体积分分数对归一化屈曲载荷的影响 ( $b=100 \text{ nm}$ ,  $h=20 \text{ nm}$ )

Fig. 5 Effect of different volume fractions on normalized buckling loads under biaxial compression ( $b=100 \text{ nm}$ ,  $h=20 \text{ nm}$ )

图 6 给出了总厚度  $h$  对两种功能梯度层合板在单轴压缩下归一化屈曲载荷影响.可以发现,两种纳米层合板的归一化屈曲载荷随着  $b/h$  值的增加而增加.这主要是因为表面面积与体积的比值随着纳米

层合板的长度和宽度的增加而增大,因此表面效应的影响增强.此外,增加总厚度  $h$  会降低归一化屈曲载荷.这是因为当增加总厚度时,表面面积与体积的比值减小,表面效应对屈曲载荷的影响减小.

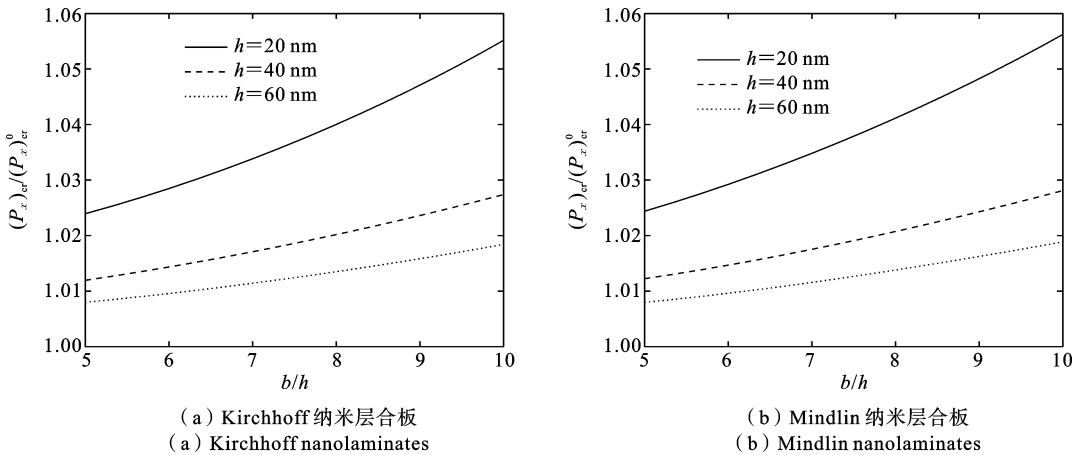


图 6 单轴压缩下不同板厚对归一化屈曲载荷的影响 ( $a=b$ ,  $h=20 \text{ nm}$ ,  $n=1$ )

Fig. 6 Effects of different plate thicknesses on normalized buckling loads under uniaxial compression ( $a=b$ ,  $h=20 \text{ nm}$ ,  $n=1$ )

图 7 给出了两种纳米层合板在双轴压缩下厚度对归一化屈曲载荷的影响.与单轴压缩类似,增加  $b/h$  值时,表面效应对双轴压缩屈曲载荷的影响增强;当增加板厚时表面效应对屈曲载荷的影响减弱.

表面效应对不同  $b/h$  值归一化屈曲载荷的影响如图 8.  $(P_x)_{cr}^K$  是 Kirchhoff 纳米层合板的临界屈曲载荷,  $(P_x)_{cr}^M$  是 Mindlin 纳米层合板临界屈曲载荷.可以看出在单轴压缩和双轴压缩的情况下,随着  $b/h$

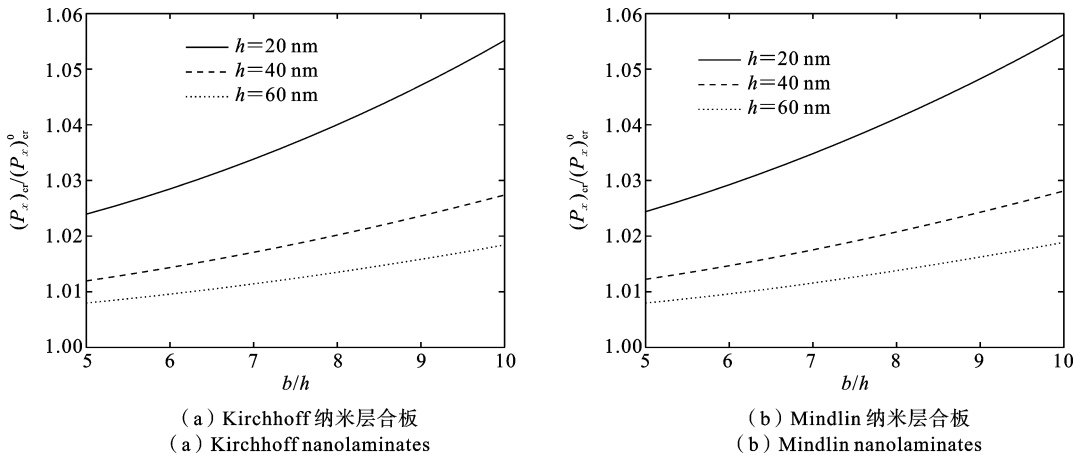


图 7 双轴压缩下不同板厚对归一化屈曲载荷的影响( $a=b, h=20 \text{ nm}, n=1$ )

Fig. 7 Effects of different plate thicknesses on normalized buckling loads under biaxial compression( $a=b, h=20 \text{ nm}, n=1$ )

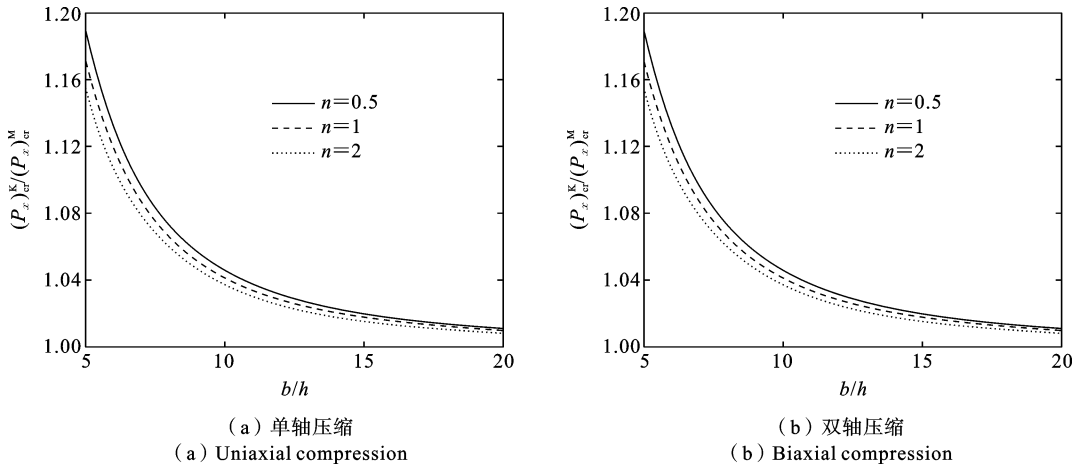


图 8 归一化屈曲载荷随  $b/h$  的变化( $a=b, h=20 \text{ nm}$ )

Fig. 8 Variations of normalized buckling loads with  $b/h$ ( $a=b, h=20 \text{ nm}$ )

值的增加,归一化屈曲载荷逐渐减小.此外,归一化屈曲载荷的比值始终大于 1,这说明考虑剪切变形会降低单轴压缩和双轴压缩的临界屈曲载荷.

### 4.3 功能梯度纳米层合板后屈曲

本节通过数值结果给出了体积分数和几何尺寸对方形功能梯度纳米层合板后屈曲行为的影响.临界后屈曲载荷通过参数  $(P_x)_{cr}^0$  归一化处理.

图 9 给出了可动边界条件下,不同体积分数对两种功能梯度纳米层合板归一化后屈曲载荷的影响.可以看到,两种纳米层合板的归一化后屈曲载荷均随着体积分数指数的增大而增加.这是因为随着组成功能梯度层合板的金属成分占比增多,表面对有效弯曲刚度的影响增强.此外,可以看出随着

板几何中心的挠度  $f$  的增大,后屈曲载荷增大.

图 10 给出了在不可动边界条件下,不同体积分数对两种纳米层合板的归一化后屈曲载荷的影响.可以观察到,与可动边界的情况类似,两种纳米层合板的归一化后屈曲载荷随着体积分数指数的增大而增加,表面效应对弯曲刚度的影响随着体积分数指数的增大而增强.两种情况的区别在于,当中心挠度为定值时,不可动边界条件下的临界载荷较可动边界条件下的临界载荷更大.

图 11 给出了在可动边界条件下,不同板厚对两种功能梯度纳米层合板的归一化后屈曲载荷的影响.可以观察到,归一化后屈曲载荷随着  $b/h$  值的增加而增大,这是因为表面效应的影响随着表面积

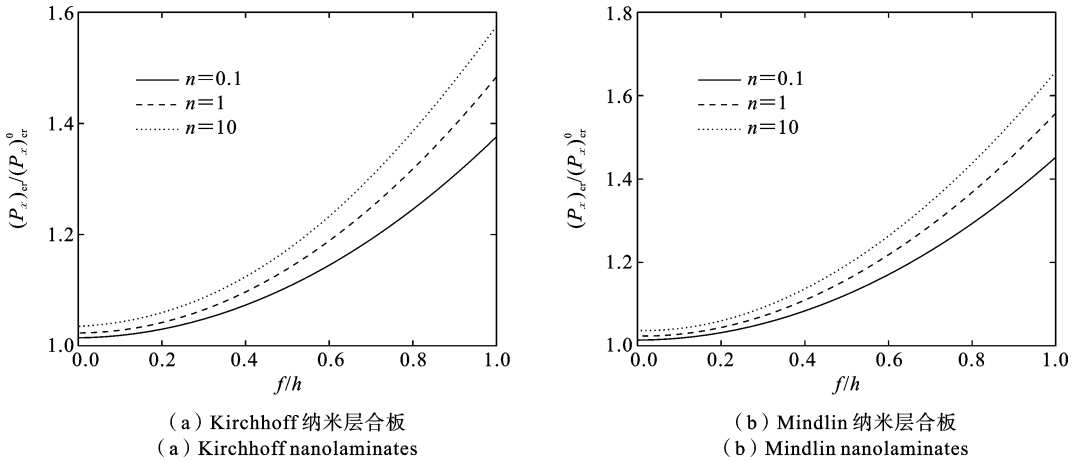


图 9 可动边界条件下体积分数对归一化后屈曲载荷的影响( $a=b=100\text{ nm}$ ,  $h=20\text{ nm}$ )

Fig. 9 Effects of volume fractions on normalized post-buckling loads under movable boundary condition ( $a=b=100\text{ nm}$ ,  $h=20\text{ nm}$ )

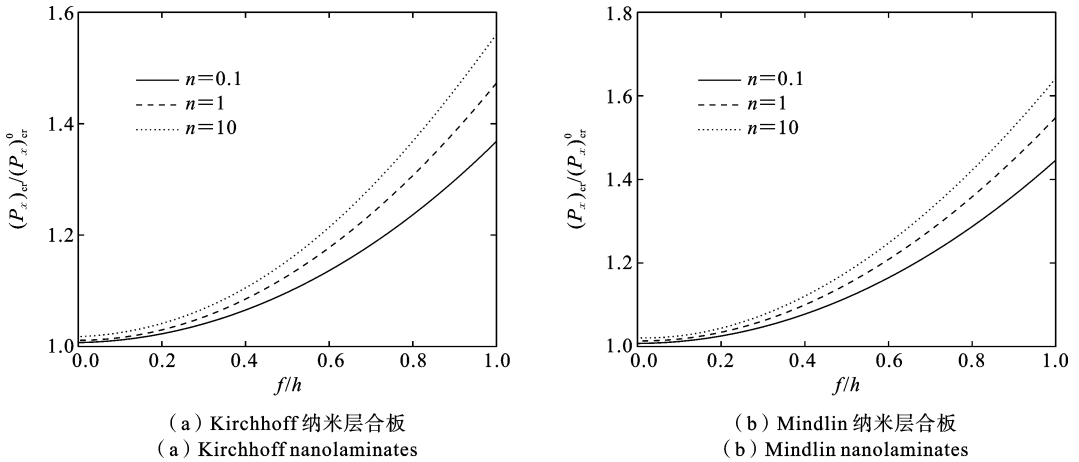


图 10 不可动边界条件下体积分数对归一化后屈曲载荷的影响( $a=b=100\text{ nm}$ ,  $h=20\text{ nm}$ )

Fig. 10 Effects of volume fractions on normalized post-buckling loads under immovable boundary conditions( $a=b=100\text{ nm}$ ,  $h=20\text{ nm}$ )

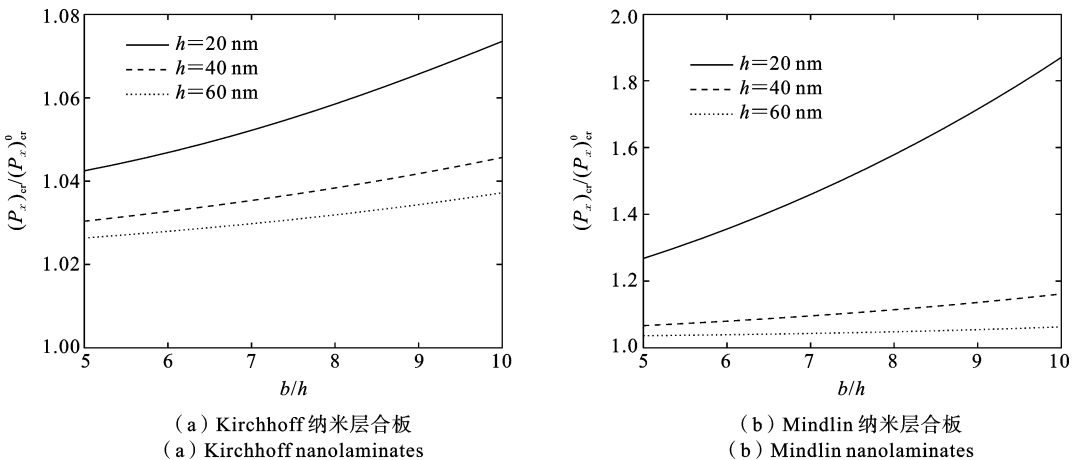


图 11 可动边界条件下板厚对归一化后屈曲载荷的影响( $a=b$ ,  $h=20\text{ nm}$ ,  $n=1$ )

Fig. 11 Effects of thicknesses on normalized buckling loads under movable boundary condition( $a=b$ ,  $h=20\text{ nm}$ ,  $n=1$ )

与体积之比的增加而增强. 此外, 增加层合板的厚度, 归一化后屈曲载荷减小, 原因是表面效应的影响随着表面面积与体积比的减小而减弱.

图 12 给出了加载边不可动边界条件下的两种功能梯度纳米层合板的厚度对归一化后屈曲载荷的影响. 由图可以看出, 与可动边界条件类似, 表面效

应对后屈曲载荷的影响随着  $b/h$  值的增加而增大, 但随着功能梯度层合板厚度的增加而减小. 此外通过对比图 12 和图 11, 可以发现不可动边界条件下的归一化后屈曲载荷大于可动边界条件下的归一化后屈曲载荷.

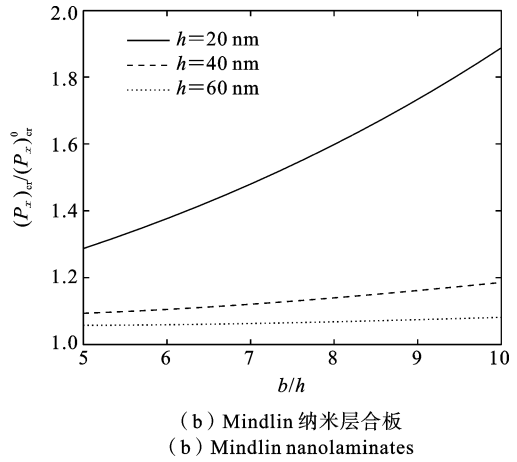
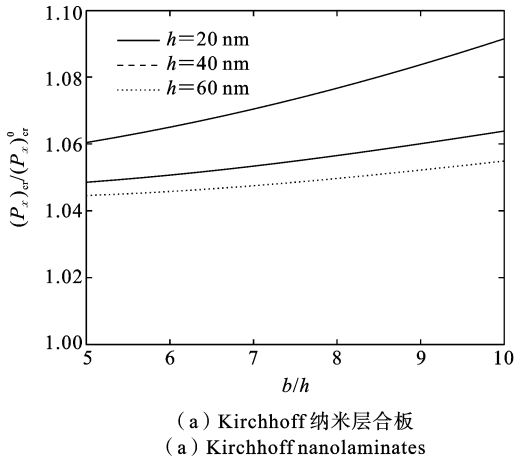


图 12 不可动边界条件下板厚对归一化后屈曲载荷的影响( $a=b, h=20 \text{ nm}, n=1$ )

Fig. 12 Effects of thicknesses on normalized buckling loads under immovable boundary condition( $a=b, h=20 \text{ nm}, n=1$ )

表面效应对具有不同  $b/h$  值的归一化后屈曲载荷影响如图 13. 参数  $(P_x)_{cr}^K$  是 Kirchhoff 纳米层合板的临界后屈曲载荷,  $(P_x)_{cr}^M$  是 Mindlin 纳米层合板临界后屈曲载荷. 由图可以看出归一化后屈曲载

荷的比值逐渐趋近于 1, 这说明考虑剪切变形会降低临界后屈曲载荷, 但随着板边长的增加, 剪切变形的影响在逐渐减弱.

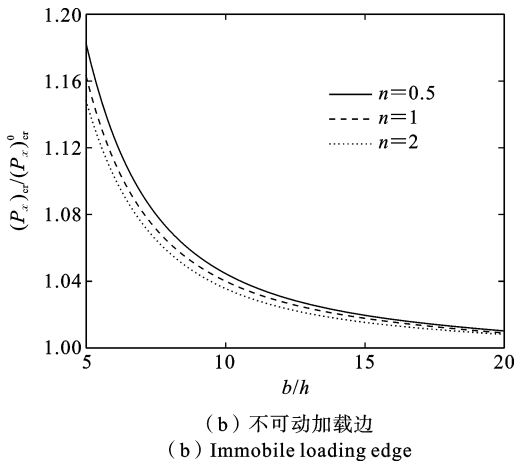
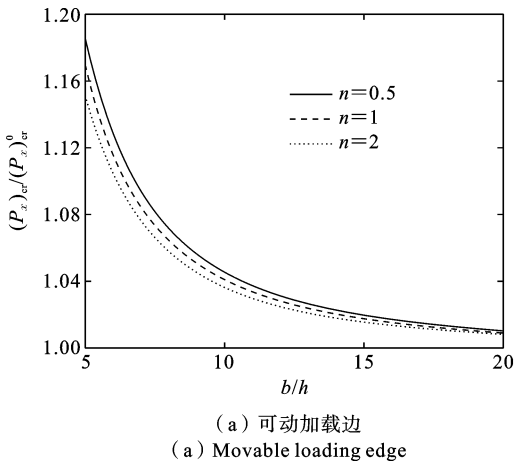


图 13 归一化后屈曲载荷随  $b/h$  的变化( $a=b, h=20 \text{ nm}, n=1$ )

Fig. 13 Variations of normalized post-buckling loads with  $b/h$ ( $a=b, h=20 \text{ nm}, n=1$ )

## 5 结论

本文利用一种考虑表面效应的功能梯度纳米层合板模型研究了表面效应对纳米层合板的屈曲和后屈曲行为的影响. 基于 Kirchhoff 板模型和 Mindlin 板模型, 通过力平衡分析, 导出了屈曲和后屈曲的控制方程. 得到了临界屈曲载荷的解析解, 并用 Galerkin 方法给出了临界后屈曲载荷近似解. 主要结论如下:

(1) 表面效应对功能梯度纳米层合板稳定性的影响与组成板材料的体积分数有关, 增大金属成分的占比, 减小陶瓷成分的占比, 会增加表面效应的影响.

(2) 表面效应对功能梯度纳米层合板稳定性的影响也与结构表面积与体积的比值有关. 增加功能梯度纳米层合板的边长, 会使表面积与体积的比值增大进而增强表面效应的影响; 增加功能梯度纳米层合板的厚度, 会使表面积与体积的比值减小进而弱化表面效应的影响.

(3) 考虑剪切变形会减小功能梯度纳米层合板的屈曲和后屈曲的临界载荷. 但是对于较薄纳米层合板, 剪切变形的影响可以忽略.

## 参考文献

- [1] Thai H T, Vo T P, Nguyen T K, et al. A nonlocal sinusoidal plate model for micro/nanoscale plates[J]. Proceedings of the Institution of Mechanical Engineers, Part C: Journal of Mechanical Engineering Science, 2014, 228(14): 2652-2660.
- [2] Karimi M, Haddad H A, Shahidi A R. Combining surface effects and non-local two variable refined plate theories on the shear/biaxial buckling and vibration of silver nanoplates[J]. Micro & Nano Letters, 2015, 10(6): 276-281.
- [3] Gurtin M E, Murdoch A I. A continuum theory of elastic material surfaces[J]. Archive for Rational Mechanics and Analysis, 1975, 57(4): 291-323.
- [4] Gurtin M E, Murdoch A I. Addenda to our paper A continuum theory of elastic material surfaces[J]. Archive for Rational Mechanics and Analysis, 1975, 59(4): 389-390.
- [5] Gurtin M E, Murdoch A I. Surface stress in solids [J]. International Journal of Solids and Structures, 1978, 14(6): 431-440.
- [6] Xu M, Wang B L, Yu A. Effect of surface and interface energies on the nonlinear bending behaviour of nanoscale laminated thin plates [J]. Mechanics of Composite Materials, 2016, 52(5): 673-686.
- [7] Barati M R, Zenkour A M. Thermal post-buckling analysis of closed circuit flexoelectric nanobeams with surface effects and geometrical imperfection[J]. Mechanics of Advanced Materials and Structures, 2019, 26(17): 1482-1490.
- [8] Abbasi F, Ghassemi A. Static bending behaviors of piezoelectric nanoplate considering thermal and mechanical loadings based on the surface elasticity and two variable refined plate theories[J]. Microsystem Technologies, 2017, 23(10): 4475-4485.
- [9] Hosseini M, Jamalpoor A, Fath A. Surface effect on the biaxial buckling and free vibration of FGM nanoplate embedded in visco-Pasternak standard linear solid-type of foundation[J]. Meccanica, 2017, 52(6): 1381-1396.
- [10] Rafieian S, Hashemian M, Pirmoradian M. Buckling analysis of double-layer piezoelectric nanoplates surrounded by elastic foundations and thermal environments considering nonlocal and surface energy models [J]. Journal of Mechanics, 2018, 34(4): 483-494.
- [11] Kamali F, Shahabian F. Analytical solutions for surface stress effects on buckling and postbuckling behavior of thin symmetric porous nano-plates resting on elastic foundation[J]. Archive of Applied Mechanics, 2021, 91(6): 2853-2880.
- [12] Kim J, Zür K K, Reddy J N. Bending, free vibration, and buckling of modified couples stress-based functionally graded porous micro-plates[J]. Composite Structures, 2019, 209: 879-888.
- [13] Ke L L, Yang J, Kitipornchai S, et al. Bending, buckling and vibration of size-dependent functionally graded annular microplates [J]. Composite Structures, 2012, 94(11): 3250-3257.
- [14] Ebrahimi F, Heidari E. Surface effects on nonlinear

- vibration of embedded functionally graded nanoplates via higher order shear deformation plate theory[J]. *Mechanics of Advanced Materials and Structures*, 2019, 26(8): 671-699.
- [15] Benveniste Y. A new approach to the application of Mori-Tanaka's theory in composite materials[J]. *Mechanics of Materials*, 1987, 6(2): 147-157.
- [16] Hill R. A self-consistent mechanics of composite materials[J]. *Journal of the Mechanics and Physics of Solids*, 1965, 13(4): 213-222.
- [17] Li K, Wu D, Chen X, et al. Isogeometric analysis of functionally graded porous plates reinforced by graphene platelets[J]. *Composite Structures*, 2018, 204: 114-130.
- [18] Sahmani S, Aghdam M M, Rabczuk T. Nonlocal strain gradient plate model for nonlinear large-amplitude vibrations of functionally graded porous micro/nano-plates reinforced with GPLs[J]. *Composite Structures*, 2018, 198: 51-62.
- [19] Duan Y, Zhang B, Li X, et al. Size-dependent elastic buckling of two-variable refined microplates embedded in elastic medium[J]. *International Journal of Applied Mechanics*, 2022, 14(04): 2250039.
- [20] 张立民, 张波, 张旭, 等. 面内压缩荷载作用下双层微板系统的同步/异步屈曲[J]. *应用数学和力学*, 2023, 44(02): 160-167. (Zhang L M, Zhang B, Zhang X, et al. Synchronous/Asynchronous buckling of double-layered microplate systems [J]. *Applied Mathematics and Mechanics*, 2023, 44(2): 160-167. (in Chinese))
- [21] Duan Y, Zhang B, Zhang X, et al. Accurate mechanical buckling analysis of couple stress-based skew thick microplates[J]. *Aerospace Science and Technology*, 2023, 132: 108056.
- [22] Li Q, Zhao X, Pan Z, et al. Nonlinear post-buckling of graded porous circular nanoplate with surface stress subjected to follower force[J]. *Mechanics of Advanced Materials and Structures*, 2024: 1-14.
- [23] Momeni-Khabisi H, Tahani M. Buckling and post-buckling analysis of double-layer magnetoelectric nano-plate strips considering piezo-flexoelectric and piezo-flexomagnetic effects[J]. *European Journal of Mechanics-A/Solids*, 2024, 104: 105218.
- [24] Vu T V, Curiel-Sosa J L, Bui T Q. A refined sin hyperbolic shear deformation theory for sandwich FG plates by enhanced meshfree with new correlation function[J]. *International Journal of Mechanics and Materials in Design*, 2019, 15(3): 647-669.
- [25] Meksi R, Benyoucef S, Mahmoudi A, et al. An analytical solution for bending, buckling and vibration responses of FGM sandwich plates[J]. *Journal of Sandwich Structures & Materials*, 2019, 21(2): 727-757.
- [26] Chi S H, Chung Y L. Mechanical behavior of functionally graded material plates under transverse load-Part I: Analysis[J]. *International Journal of Solids and Structures*, 2006, 43(13): 3657-3674.
- [27] Mahmoud F F, Shaat M. A new mindlin FG plate model incorporating microstructure and surface energy effects[J]. *Structural Engineering and Mechanics*, 2015, 53(1): 105-130.
- [28] He J, Lilley C M. Surface effect on the elastic behavior of static bending nanowires[J]. *Nano Letters*, 2008, 8(7): 1798-1802.
- [29] Wang G F, Feng X Q. Timoshenko beam model for buckling and vibration of nanowires with surface effects[J]. *Journal of Physics D: Applied Physics*, 2009, 42(15): 155411.
- [30] Wang K F, Wang B L, Xu M H, et al. Influences of surface and interface energies on the nonlinear vibration of laminated nanoscale plates [J]. *Composite Structures*, 2018, 183: 423-433.
- [31] Sapsathiarn Y, Rajapakse R. Static and dynamic analyses of nanoscale rectangular plates incorporating surface energy[J]. *Acta Mechanica*, 2017, 228(8): 2849-2863.
- [32] Yan Z, Jiang L Y. Vibration and buckling analysis of a piezoelectric nanoplate considering surface effects and in-plane constraints[J]. *Proceedings of the Royal Society A: Mathematical, Physical and Engineering Sciences*, 2012, 468(2147): 3458-3475.
- [33] Ansari R, Shahabodini A, Shojaei M F, et al. On the bending and buckling behaviors of Mindlin nanoplates considering surface energies[J]. *Physica E: Low-Dimensional Systems and Nanostructures*, 2014, 57: 126-137.

- [34] Wang K F, Wang B L. Effect of surface energy on the non-linear postbuckling behavior of nanoplates [J]. *International Journal of Non-Linear Mechanics*, 2013, 55: 19-24.
- [35] Ansari R, Ashrafi M A, Pourashraf T, et al. Vibration and buckling characteristics of functionally graded nanoplates subjected to thermal loading based on surface elasticity theory[J]. *Acta Astronautica*, 2015, 109: 42-51.
- [36] Wang J, Xiao J H, Xia X D. Buckling and post-buckling behavior of nano-laminates considering surface effects[J]. *Archive of Applied Mechanics*, 2024, 94 (11): 3469-3488.
- [37] Wang K F, Wang B L. Effect of surface energy on the non-linear postbuckling behavior of nanoplates [J]. *International Journal of Non-Linear Mechanics*, 2013, 55: 19-24.

## Buckling and Post-buckling of Functionally Graded Sandwich Nanoplates with Surface Effect

Junhua Xiao<sup>1,2</sup>     Jie Wang<sup>1,2,3,4</sup>

*(<sup>1</sup>Department of Engineering Mechanics, Yanshan University, Qinhuangdao, 066004)*

*(<sup>2</sup>Hebei Key Laboratory of Mechanics Reliability for Heavy Equipment and Large Structures, Yanshan University, Qinhuangdao, 066004)*

*(<sup>3</sup>State Key Laboratory of Nonlinear Mechanics (LNM), Institute of Mechanics, Chinese Academy of Sciences, Beijing, 100190)*

*(<sup>4</sup>School of Engineering Science, University of Chinese Academy of Sciences, Beijing, 100049)*

**Abstract** Nanoplate structures are widely used in nanoelectromechanical systems because of their excellent mechanical properties. At the same volume, the specific surface area of the nano-laminates is much larger than that of the single-layer nanomaterials, and the surface effect is more significant. The influence of the surface effect on nanostructures can be regarded as the combination of surface elasticity and surface residual stress. The classical plate-shell theory does not consider the surface effect and is no longer suitable for describing nanostructures such as nanoplate-shells. As a new type of composite materials, functionally graded materials have received more and more attention from researchers. The mechanical properties of micro/nano structural components made of functionally graded materials are completely different from the macroscopic structures made of conventional materials. Plate structure is a basic component in nanoelectromechanical systems, so it is necessary to study the mechanical properties of plates made of functionally graded materials. In this paper, based on Kirchhoff plate theory and Mindlin plate theory considering shear deformation, the buckling and post-buckling behaviors of functionally graded sandwich nanoplates with surface effect are studied. Based on the force balance analysis, the governing equations of buckling and post-buckling are obtained. The analytical solutions of critical buckling loads under uniaxial and biaxial compression are given. By using the Galerkin method, the approximate solutions of critical post-buckling loads under movable and immovable boundary conditions are given. Numerical results show that the influence of surface effects on the stability of functionally graded nano-laminated plates is related to the volume fraction of the materials that make up the plates, as well as to the ratio of structural surface area to volume. Considering that shear deformation will reduce the critical load for buckling and post-buckling of functionally graded nano-laminated plates, the influence of shear deformation can be ignored for thinner nano-laminated plates.

**Key words** surface effect, functionally graded material, rectangular laminate, buckling, post-buckling